LAMINAR BOUNDARY LAYER WITH A PRECIPITATING DISPERSE IMPURITY

V. A. Naumov

UDC 532.529

The finite differences method is used to numerically study the structure of a laminar boundary layer with a precipitating disperse impurity on a semiinfinite plate.

The precipitation of a disperse impurity on the walls of a channel is generally studied on single particles in a given field of gas velocities (see [1,2], for example). Such an approach is valid only for very low concentrations of the disperse phase, since it does not permit consideration of the effect of the disperse particles on the dispersion medium. Here, we examine a laminar boundary layer with a monodisperse mixture precipitating on a semiinfinite plate in the case of a zero pressure gradient. The volume fraction of the impurity is much less than the volume fraction of the dispersion medium but is comparable in the terms of the mass fraction. In cases where the concentrations of the impurity is substantial, it is expedient to use the theory of interpenetrating continua [3]. The system of equations of the boundary layer of a two-phase medium on a plate was formulated in [4-6] within the framework of this theory (also see the bibliography in [5,6]). However, it was assumed in [4-6] that only aerodynamic resistance acted on the disperse particles. Besides this force, the authors of [7] considered the Magnus force due to rotation of the particles. The authors of [7] spoke of the "motion of moisture in the through parts of steam turbines," but the calculated profiles of ρ_p and v_p did not correspond to precipitation problems. The Safman force was not even mentioned in [7], and the results of the calculations were presented without an indication of the dimensions or density of the disperse impurity.

Since we are examining a laminar boundary layer or a semiinfinite plate, we choose U_e as the velocity scale, ν/U_e as the length scale, and R^o as the density scale. The gas phase is assumed to be incompressible, $\alpha_p \sim 10^{-3}$. It follows from this that $R = (1 - \alpha_p) R^o \approx R^o = \text{const}$. At $\partial p_e/\partial x = 0$, with allowance for $R^o/R_p{}^o \ll 1$, the system of equations of a boundary layer with rotating monodisperse particles of an impurity can be written in the following dimensionless form:

$$\frac{\partial u}{\partial x} + \frac{\partial v}{\partial y} = 0, \tag{1}$$

$$\frac{\partial}{\partial x}(\rho_p u_p) + \frac{\partial}{\partial y}(\rho_p v_p) = 0, \tag{2}$$

$$u\frac{\partial u}{\partial x} + v\frac{\partial u}{\partial y} = \frac{\partial^2 u}{\partial y^2} - \rho_p f_x, \tag{3}$$

$$u_p\frac{\partial u_p}{\partial x} + v_p\frac{\partial u_p}{\partial y} = f_x, \tag{4}$$

$$u_p\frac{\partial v_p}{\partial x} + v_p\frac{\partial v_p}{\partial y} = f_y, \tag{5}$$

$$u_p\frac{\partial \omega_p}{\partial x} + v_p\frac{\partial \omega_p}{\partial y} = -\frac{10}{3\,\mathrm{Stk}}\left(\omega_p + \frac{1}{2}\frac{\partial u}{\partial y}\right). \tag{6}$$

Here and below, the subscript p denotes parameters pertaining to the disperse phase, while the absence of subscripts denotes parameters pertaining to the dispersion medium. The dimensionless coordinates x and y are the corresponding Reynolds numbers.

Kaliningrad Engineering Institute of the Fishing Industry. Translated from Inzhenerno-Fizicheskii Zhurnal, Vol. 55, No. 4, pp. 559-565, October, 1988. Original article submitted May 18, 1987.

 0003-6838/88/2401-1092$12.50 © 1989 Plenum Publishing Corporation

It is necessary to assign boundary conditions on the wall and in the external flow for the system of equations. We also need to assign the profiles of the unknowns with a certain coordinate x_0. At $y \to \infty$ $u = 1$, $u_p = u_{pe}$, $v_p = 0$, $\rho_p = \rho_{pe}$, $\omega_p = 0$, i.e., the flow about the plate is plane-parallel and contains nonrotating disperse particles. No boundary conditions for the precipitating disperse phase are assigned on the plate (at $y = 0$); the boundary conditions for the dispersion medium $u_w = v_w = 0$.

It was shown in [6] that the phases do not interact at a distance x_0 which is much less than the particle stagnation length L. Here, we assigned the initial profiles with $X_0/L = 0.02$. For the disperse phase, these profiles do not differ from the parameters in the incoming flow: $u_{p0} = u_{pe}$, $\rho_{p0} = \rho_{pe}$, $v_{p0} = 0$, $\omega_{p0} = 0$. The dynamics of the dispersion medium at $X \ll L$ is described by the Navier–Stokes equations for a one-phase flow. We note that

$$x_0 \equiv \mathrm{Re}_{x0} = \frac{\mathrm{Re}_d^2}{24\lambda}\,\frac{X_0}{L}\,.$$

Since $\lambda = 0.00075$ and $\mathrm{Re}_d \geq 10$ in the present study, then $x_0 > 100$. Thus, the Prandtl equations describing a one-phase laminar boundary layer are valid for the dispersion medium at $x = x_0$. As in [6], as the initial profiles of the dispersion medium we assigned the well-known Blausius solution.

Apparent additional mass, buoyancy, and the Basse force can be ignored in gas suspensions. We further assume that forces of an electrostatic or thermophoretic nature are absent and that the Froude numbers are such that gravity can be ignored.

Let us determine the aerodynamic resistance acting on a single disperse particle:

$$\mathbf{F}_\mu = \frac{1}{2_j}\, c_d R^\circ\, \frac{1}{4}\, \pi d^2\, |\mathbf{V}_r|\, \mathbf{V}_r, \quad \mathbf{V}_r = \mathbf{V} - \mathbf{V}_p.$$

The method in [8] can be used to determine the resistance coefficient of a spherical particle within a broad range of Reynolds numbers Re_p; then, assuming that $f_\mu = \nu F_\mu/(m_p U_e{}^3)$, we obtain

$$f_{\mu x} = \gamma(u - u_p), \quad f_{\mu y} = \gamma(v - v_p), \quad \gamma = (1 + 0{,}179\mathrm{Re}_p^{1/2} + 0{,}013\mathrm{Re}_p)/\mathrm{Stk}.$$

The buoyant Magnus force is due to the rotation of the particles and is determined as follows [3]

$$\mathbf{F}_M = \frac{1}{6}\, c_M\, \pi d^3 R^\circ [\mathbf{V}_r \times \boldsymbol{\Omega}_p]. \tag{7}$$

Considering $c_M = 3/4$ for small Re_p and small Re_ω, it follows from [7] that

$$f_{Mx} = \lambda\omega_p(v - v_p), \quad f_{My} = -\lambda\omega_p(u - u_p). \tag{8}$$

It was assumed in [7] that the angular velocity of the disperse particle is equal to the angular velocity of the fluid element surrounding it. However, a plus sign was used in the expression $\omega_p = -0.5\,\partial u/\partial y$, i.e. an error was made in the sign of the Magnus force.

We propose that the Safman force can be approximately determined by the same expression as in the case of the steady gradient flow of a viscous incompressible fluid about a single slowly rotating sphere [3]:

$$F_S = 1{,}61 R^\circ \nu^{1/2} d^2 (U - U_p) \left(\frac{\partial U}{\partial Y}\right)^{1/2}, \tag{9}$$

$$f_S = 4{,}1\, \frac{\lambda}{\mathrm{Re}_d}\, (u - u_p) \left(\frac{\partial u}{\partial y}\right)^{1/2}. \tag{10}$$

In a formula in [2] which is similar to (9), an error was also made in the sign and the coefficient was exaggerated by a factor of 4π. Thus, according to the calculations that were performed, disperse particles which had penetrated the boundary layer were forced out of the layer by the Safman force – although it is clear from Eq. (10) that, in the problem being considered, the Safman force will facilitate precipitation of the disperse phase.

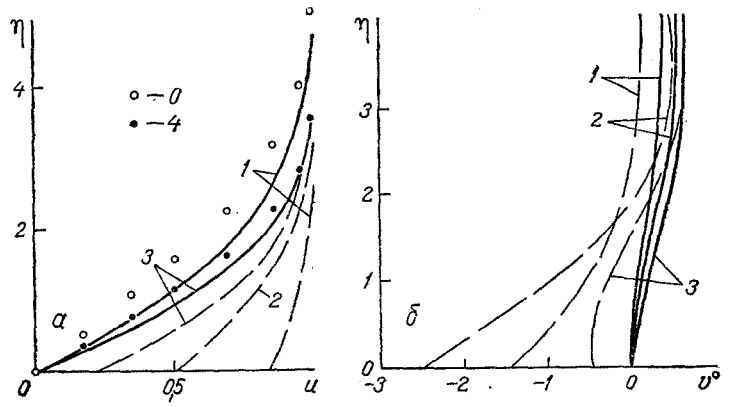

Fig. 1. Profiles of dimensionless longitudinal (a) and transverse (b) velocities of the dispersion medium (solid curves) and disperse phase (dashed curves) at $Re_d = 10$: a) 1) $10^{-5} \cdot Re_x = 0.01$; 2) 0.055; 3) 0.22; points denote the longitudinal velocity of the gas in the Blasius similarity solution: 0) in relation to the argument η; 4) in relation to the argument ξ: b) 1) $10^{-5} \cdot Re_x = 0.02$; 2) 0.11; 3) 0.55. Here and below, $\lambda = 0.00075$, $u_{pe} = 1$, $\rho_{pe} = 1$.

Let us compare the Safman force and a projection of the Magnus force on the transverse axis:

$$\beta = \left|\frac{f_{My}}{f_S}\right| = \frac{|\omega_p| \, Re_d}{4{,}1\,(\partial u/\partial y)^{1/2}} \leqslant \frac{Re_d}{8{,}2}\left(\frac{\partial u}{\partial y}\right)^{1/2}.$$

The inequality is valid for precipitation problems not involving the rebound of particles from the wall at a high velocity. Using the one-phase Blausius solution $\partial u/\partial y \leq 0.332/\sqrt{x}$ as an estimate – where equality is attained only at the wall – we finally obtain

$$\beta \leqslant 0{,}07 Re_d/\sqrt[4]{Re_x}. \qquad (11)$$

It follows from inequality (11) that, in precipitation problems, the Magnus force can be ignored when the ratio $Re_d/\sqrt[4]{Re_x}$ is small.

Considering that the Stokes number can be represented in the form $Stk = Re_d^2/(24\lambda)$ and taking (8) and (10) into account, we note that the similiarity criteria of the problem in question are the ratio of the true densities of the phases λ and the Reynolds number, the latter being determined from the particle diameter and the gas velocity in the external flow Re_d.

To solve the formulated problem, we used variables $\eta = y/\sqrt{x}$, $v^o = \sqrt{x}v$, $v_p{}^o = \sqrt{x}v_p$ and a difference grid which was refined near the wall in accordance with the geometric progression $\Delta\eta_{m+1} = \Delta\eta_m/z$, where $m = 1, 2, \ldots, M_1$; $z = 0.85$, $m_1 = 1$ corresponds to a node on the plate, $M_1 = 26$ corresponds to a node on the external boundary.

The difference scheme we chose to use on this grid had the property of strongly stabilizing high-frequency perturbations, similar to the scheme described in [9]. Here, artificial viscosity was used in the difference analogs of the equations of the disperse phase (4-6). The first preliminary values of the unknowns $\bar{u}$, $\bar{\varphi} = (u_p, v_p, u_p)$ were determined for the layer $(n + 1)$. We then used an explicit running-count scheme to calculate the values of $v_m{}^{n+1/2}$, $\rho_{pm}{}^{n+1/2}$. The second preliminary values of the unknowns $\bar{\bar{u}}$, $\bar{\bar{\varphi}}$ were determined in two stages – first, on the half-integral layer $(n + 1/2)$ with the step $\Delta x/2$, and then with the same step on the layer $(n + 1)$. Finally, we determined $\varphi_m^{n+1} = 2\bar{\bar{\varphi}}_m^{n+1} - \bar{\varphi}_m^{n+1}$.

The scheme we employed, with central-difference approximation of the derivative with respect to η, requires additional boundary conditions that were not included in the boundary-value problem in [9]. The additional conditions for the disperse phase on the plate $\varphi_1{}^{n+1}$ are obtained in explicit form from the corresponding equations. The system of difference equations and the corresponding boundary conditions were solved by trial run.

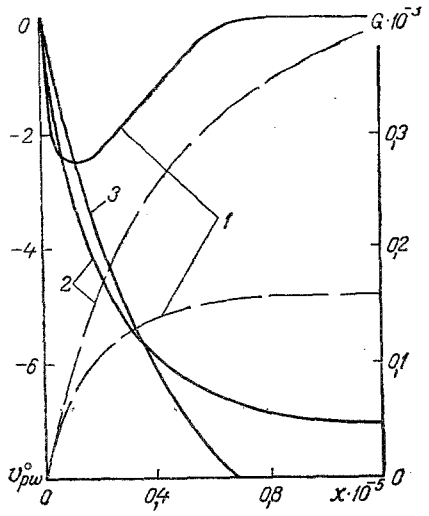

Fig. 2

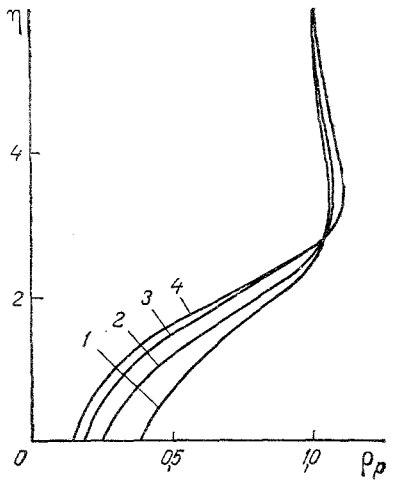

Fig. 3

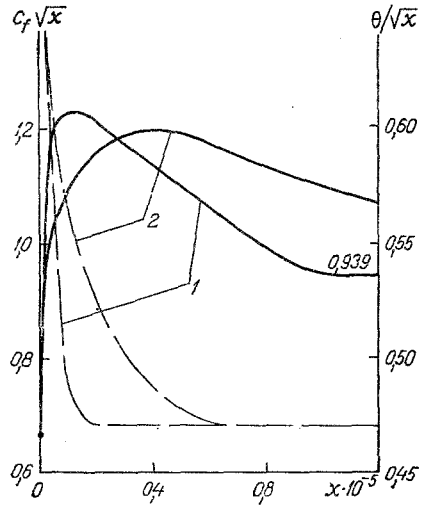

Fig. 4

Fig. 2. Change in the transverse velocity of the impurity on the plate (solid lines) and the integral flux of the precipitating impurity (dashed lines): 1) Re_d = 10; 2) 20; 3) 50.

Fig. 3. Profiles of the distributed density of the impurity at Re_d = 10: 1) $10^{-5}\cdot Re_x$ = 0.03; 2) 0.055; 3) 0.11; 4) 0.33.

Fig. 4. Change in the local resistance coefficient (solid curves) and momentum thickness (dashed curves) along the plate: 1) Re_d = 10; 2) Re_d = 20.

If we integrate Eq. (2) and the sum of Eqs. (3) and (4) – with allowance for $v_{pe} = 0$ – across the boundary layer, the resulting integrals can be used to check the accuracy of the calculations:

$$\int_0^\infty \rho_p u_p dy = G_0 + G_w, \quad G_w = \int_0^x \rho_{pw} v_{pw} dx,$$

$$\int_0^\infty u(1-u)\,dy + \int_0^\infty \rho_p u_p (1-u_p)\,dy = I_0 + \int_0^x \frac{\partial u}{\partial y}\,dx + \int_0^x \rho_{pw} v_{pw} (1-u_{pw})\,dx. \tag{12}$$

The last terms characterize the mass and momentum losses of the disperse phase due to precipitation. In calculations performed by the method described above, Eqs. (12) were satisfied with an error of 3-4%.

Figure 1 shows results of calculations of the velocity profiles of the phases in the laminar boundary layer along the plate. The problem is known [6] to have a similarity solution in the region which is an equilibrium region with respect to phase velocity ($x \to \infty$). The profile of longitudinal velocity, meanwhile, coincides with the Blasius profile of the argument $\xi = \eta(1 + \rho_{pe})^{1/2}$. It is evident from Fig. 1a that the profiles of longitudinal velocity become more and less full, respectively, for the dispersion medium and the disperse phase as x increases. This can be attributed to the exchange of momentum between the phases due to aerodynamic resistance. The fullness of the velocity profile of the dispersion medium at $x > 0.02 \cdot 10^5$ exceeds the fullness of the Blasius profile of the argument ξ; at $x > 0.2 \cdot 10^5$, the profiles of the constituent phases continue to approach one another and become less full, tending toward the above-indicated Blasius profile.

The change in the profiles of the transverse velocity of the disperse phase in the region which is nonequilibrium with respect to phase velocity differs considerably from the change seen in [6] without allowance for the buoyancy forces acting on the particle. As can be seen from Fig. 1a, in the nonequilibrium region, the longitudinal velocity of the disperse phase is greater than the longitudinal velocity of the gas. The largest difference in longitudinal velocities is seen at the wall, and it is here that $\partial u/\partial y$ attains its largest value. Thus, in accordance with Eqs. (8) and (10), both the Safman force and the projection of the Magnus force on the transverse axis are negative. As a result, in the wall region in Fig. 1b, the transverse velocity of the disperse phase is directed toward the wall. Away from the wall, where buoyancy is small, the transverse velocities of the disperse phase and the gas are both positive. At $x \to \infty$, $v_p \to v$, i.e., $v_p > 0$ (as for the dispersion medium), while $v_{pw} = v_w = 0$ on the wall.

Figure 2 shows the change in the transverse velocity of the disperse phase on the plate. The modulus v_{pw} begins to increase near the leading edge of the plate and then decreases, since the quantity $u_p - u$ also decreases. After having reached a minimum (at $x \approx 0.125 \cdot 10^5$), at $Re_d = 10$ the quantity v_{pw} becomes negligible at the distance $x > 0.8 \cdot 10^5$. An increase in Re_d leads to a situation whereby the modulus v_{pw} increases less rapidly along x but still reaches large values. Here, the nonequilibrium region becomes more extensive. Calculations performed for $Re_d \geq 50$ showed that the flow remains essentially nonequilibrium with respect to phase velocities right up to the region where the transition occurs from a laminar boundary layer to turbulent flow.

Figure 3 shows calculated profiles of the concentration of the disperse phase. Since the transverse velocity of the particle is negative in the wall region, it settles out onto the plate. As a result of this precipitation, the impurity concentration is lower near the wall than in the incoming flow; the concentration continues to decrease with increasing distance from the leading edge of the plate as long as the value of $v_{pw} < 0$ remains substantial. Downflow, as $v_{pw} \to 0$, the impurity concentration in the wall region begins to increase; the concentration profiles have their largest values at the wall. The author of [6] obtained such concentration profiles over the entire flow region (except for the distant equilibrium zone), since buoyancy was not considered. In [7], the above-noted error in the sign of the Magnus force and the absence of the Safman force led to a situation whereby the transverse velocity of the particle $v_p > 0$ in the wall zone, particle precipitation was absent, and there was no reduction in impurity concentration near the plate due to precipitation. At $\eta \geq 2.5$, Fig. 3 shows a zone with a high impurity concentration $\rho_p > \rho_{pe}$. It is evident from Fig. 1b that, here, $v_p > 0$. However, since $v_{pe} = 0$, then this zone receives some of the impurity present in the wall region.

The study [4] presented graphs of the change in the thickness of a laminar two-phase boundary layer. The thickness of the two-phase layer was greater than the thickness of the one-phase layer. However, it is evident from Fig. 1a that the distance from the plate at which the longitudinal velocity of the gas differs from U_e by 1% (as an example) is shorter in the two-phase flow. Figure 4 shows the effect of the disperse phase on the local friction coefficient and the momentum thickness of the laminar boundary layer. In the initial section $c_f\sqrt{x} = 0.664$; $\theta/\sqrt{x} = 0.664$, as in the one-phase case. In the region which is equilibrium with respect to phase velocities [6]: $c_f\sqrt{x} \to 0.664(1 + \rho_{pe})^{1/2}$, $\theta/\sqrt{x} \to 0.664/(1 + \rho_{pe})^{1/2}$. The lower the value of Re_d, the more rapid the local friction coefficient and momentum thickness reach their respective limiting values. Here, the equilibrium value of the integral characteristic $\theta/\sqrt{x}$ is reached considerably earlier than that of the differential characteristic $c_f\sqrt{x}$.

The proposed method of calculation makes it possible to evaluate both the local and the integral rate of precipitation of a disperse impurity in a laminar boundary layer. Figure 2 shows results of calculation of the integral G_w. The integral flux increases as long as v_{pw} has large negative values. A reduction in v_{pw} – in addition to the reduction in ρ_{pw} downflow (Fig. 3) – leads to a slowing of the increase in G_w. In the equilibrium (with respect to phase velocity) region, G_w = const, since $v_{pw} = 0$ and no precipitation occurs. With an increase in Re_d, precipitation intensifies due to the large values of v_{pw}.

NOTATION

$x = XU_e/\nu \equiv Re_x$; $y = YU_e/\nu \equiv Re_y$; X, Y, longitudinal and transverse coordinates; $\eta = y/\sqrt{x}$; ν, kinematic viscosity of the gas; $u = U/U_e$, $v = V/U_e$, dimensionless longitudinal and transverse components of velocity; $\rho_p = R_p/R^o$; R_p, R, distributed densities of the impurity and dispersion medium; $\lambda = 0.75R^o/R_p^o$; R^o, R_p^o, true densities of the phases; α, α_p, volume fractions of the phases; $f = F\nu/(m_pU_e^3)$; F, phase interaction force; m_p, mass of a disperse particle; $L = U_ed^2/(24\lambda\nu)$, particle stagnation length; $\omega_p = \Omega_p\nu/U_e^2$, dimensionless angular velocity of a particle; c_f, local resistance coefficient of the plate; $p = P/(R^oU_e^2)$, dimensionless pressure; $Stk = R_p{}^od^2U_e^2/(18R^o\nu^2)$, Stokes number; $Re_p = V_rd/\nu$, $Re_d = U_ed/\nu$, $Re_\omega = \Omega_pd^2/\nu$, Reynolds numbers; d, diameter of disperse particle; $\theta \equiv Re_\theta$, dimensionless momentum thickness; G_w, integral flux of impurity precipitating on the plate. Indices: p, disperse impurity, w, plate, e, external flow; 0, initial section.

LITERATURE CITED

1. Roukhainen and Stashevich, Teploperedacha, 92, No. 1, 118-127 (1970).
2. I. D. Larionov and N. I. Syromyatnikov, Inzh.-Fiz. Zh., 23, No. 4, 646-649 (1972).
3. R. I. Nigmatulin, Principles of the Mechanics of Heterogeneous Media [in Russian], Moscow (1978).
4. W. Tabakoff and A. Hamed, Z. Fluggwiss., 20, No. 10, 373-380 (1972).
5. V. P. Stulov, Izv. Akad. Nauk SSSR, Mekh. Zhidk. Gaza, No. 1, 51-60 (1979).
6. A. N. Osipov, Izv. Akad. Nauk SSSR, Mekh. Zhidk. Gaza, No. 4, 48-54 (1980).
7. L. I. Seleznev and L. A. Ignatevskaya, Problems of Improving and Studying Turbines: Collection of Scientific Transactions, Moscow Energy Institute, Moscow, No. 306, 20-24 (1976).
8. L. B. Gavin and V. A. Naumov, Inzh.-Fiz. Zh., 44, No. 3, 927-932 (1983).
9. V. M. Paskonov, V. I. Polezhaev, and L. A. Chudov, Numerical Study of Heat and Mass Transfer Processes [in Russian], Moscow (1984).